Energy Transfer in Dendritic Macromolecules: Molecular Size Effects and the Role of an Energy Gradient

ARTICLE *in* JOURNAL OF THE AMERICAN CHEMICAL SOCIETY · OCTOBER 1996

Impact Factor: 12.11 · DOI: 10.1021/ja961418t

3 AUTHORS, INCLUDING:

Chelladurai Devadoss
University of Illinois, Urbana-Champaign
26 PUBLICATIONS **3,028** CITATIONS

SEE PROFILE

Jeffrey S Moore
University of Illinois, Urbana-Champaign
424 PUBLICATIONS **26,528** CITATIONS

SEE PROFILE

Energy Transfer in Dendritic Macromolecules: Molecular Size Effects and the Role of an Energy Gradient

Chelladurai Devadoss, P. Bharathi, and Jeffrey S. Moore*

Contribution from the Roger Adams Laboratory, Department of Chemistry, Materials Science & Engineering, and the Beckman Institute for Advanced Science and Technology, University of Illinois at Urbana-Champaign, Urbana, Illinois 61801

Received April 29, 1996[⊗]

Abstract: Perylene-terminated monodendrons **1**−**7** and phenyl-terminated reference monodendrons **8**−**14** have been synthesized, and the intramolecular energy transfer has been studied using steady-state as well as time-resolved fluorescence spectroscopy. In the series **2**−**7**, the light-harvesting ability of these compounds increases with increasing generation due to the increase in molar extinction coefficient. However, the efficiency of the energy transfer decreases with increasing generation in this series. With increasing generation, the photoluminescence intensity from the perylene core still increases and the expected level-off in the photoluminescence intensity has not been reached in this series of compounds. Dendrimer **1** is unique in that the energy transfer in this molecule occurs at a very fast rate. The rate constant for energy transfer in **1** is at least 2 orders of magnitude larger than in **2**−**7**. In contrast to monodendrons **2**−**7**, **1** possesses a variable monomer type at each generation that creates an energy funnel. The ultrafast energy transfer in this system is best explained by the presence of this energy gradient.

Introduction

Excitation energy transfer plays an important role in natural phenomena such as photosynthesis.[1,2] In the natural photosynthetic unit in plants, carotenoids, acting as antennas, absorb solar radiation in the spectral region where the chlorophyll molecules absorb weakly and transfer the resulting excitation energy to chlorophyll via singlet−singlet energy transfer.[3−5] The excitation energy then migrates from one chlorophyll molecule to another unidirectionally in an array and ultimately reaches the special pair in the reaction center where charge separation occurs. Recent structural studies on bacterial photosynthetic units highlight the importance of an energy gradient for the efficient energy transfer in these systems.[6] The photosynthetic unit consists of an outer antenna complex (light-harvesting complex two, LH2), an inner antenna complex (light-harvesting complex one, LH1), and the reaction center. LH1 is red-shifted with respect to LH2, and therefore LH1 serves as an energy funnel for the reaction center, which is lower in energy than both LH1 and LH2. Furthermore, carotenoids provide photoprotection to chlorophyll molecules by intercepting the chlorophyll triplet states which are formed in the antenna system or reaction center. This triplet−triplet energy transfer prevents chlorophyll-sensitized generation of singlet oxygen, which is harmful to the organism.[7−9]

In addition to its importance in natural processes, excitation energy transfer finds application in such varied phenomena as photodegradation and photostabilization of polymers where the radiation energy absorbed by the polymer backbone is transferred to the stabilizer (quencher) which quickly dissipates the energy by some efficient nonradiative processes.[10,11] In biology, singlet−singlet energy transfer is frequently employed as a means to measure the interchromophore distances in proteins, nucleic acids, and other biomacromolecules.[12] Applying nonradiative energy transfer measurements, Haas probed the dynamics of protein folding using fluorescence-labeled peptides.[13] This process is also important in such diverse areas like rare-earth-metal-doped lasers,[14] photosensitized organic reactions,[15] and plastic scintillators.[16]

Of late there has been a widespread interest in the research to mimic the natural photosynthesis process, both the energy transfer as well as the charge transfer aspects of it.[17,18] Many molecular devices have been constructed to harvest solar energy and to utilize the energy to effect other chemical reactions. Guillet and co-workers made what they call "photozymes", a short term for photochemical enzymes.[19] These photozymes are polyelectrolytes made from mixtures of hydrophobic and hydrophilic comonomers. They contain photon-harvesting chromophores which transport excitation energy to organic substrates buried deep in the interior of the macromolecular coil for further chemical reactions. Gust et al. made a series of carotenoporphyrin dyads to examine the energy transfer aspect

* To whom correspondence should be addressed at the Roger Adams Laboratory, Department of Chemistry, Materials Science and Engineering.

[⊗] Abstract published in *Advance ACS Abstracts,* September 1, 1996.

(1) Knox, R. S. In *Primary Processes of Photosynthesis*; Barber, J., Ed.; Elsevier: Amsterdam, 1977; Vol. 2.
(2) Deming-Adams, B. *Biochim. Biophys. Acta* **1990**, *1020*, 1.
(3) Goedheer, J. D. *Biochim. Biophys. Acta* **1969**, *172*, 252.
(4) Cogdell, R. J.; Frank, H. A. *Biochim. Biophys. Acta* **1987**, *895*, 63.
(5) McDermott, G.; Prince, S. M.; Freer, A. A.; Hawthornthwaite-Lawless, A. M.; Papiz, M. Z.; Cogdell, R. J.; Isaacs, N. W. *Nature* **1995**, *374*, 517.
(6) Kuhlbrandt, W. *Nature* **1995**, *374*, 497.
(7) Foote, C. S.; Chang, Y. C.; Denny, R. W. *J. Am. Chem. Soc.* **1970**, *92*, 5216.
(8) Monger, T. G.; Cogdell, R. J.; Parson, W. W. *Biochim. Biophys. Acta* **1976**, *449*, 136.
(9) Davidson, E.; Cogdell, R. J. *Biochim. Biophys. Acta* **1981**, *635*, 295.
(10) Jellinek, H. H. G. *Degradation and Stabilization of Polymers*; Elsevier: Amsterdam, 1991; Vol. 2.
(11) Pappas, S. P.; Winslow, F. H. *Photodegradation and Photostabilization of Coatings*; American Chemical Society: Washington, DC, 1981.
(12) Stryer, L. *Annu. Rev. Biochem.* **1978**, *47*, 819.
(13) Winnik, M. *Photophysical and Photochemical Tools in Polymer Science*; D. Reidel Publishing Co.: Dordrecht, The Netherlands, 1986.
(14) Macfarlane, R. M.; Shelby, R. M. *J. Lumin.* **1987**, *36*, 179.
(15) Turro, N. J. *Modern Molecular Photochemistry*; Benjamin-Cummings Publishing Co.: Menlo Park, CA, 1981.
(16) Swank, R. K.; Buch, W. L. *Phys. Rev.* **1953**, *91*, 927.
(17) Gust, D.; Moore, T. A. *Adv. Photochem.* **1991**, *16*, 1.
(18) Gust, D.; Moore, T. A.; Moore, A. *Acc. Chem. Res.* **1993**, *26*, 1.
(19) Guillet, J. E.; Burke, N. A. D.; Nowokowska, M.; Reese, H.; Gravett, D. M. *Macromol. Symp.* **1995**, *98*, 53.

S0002-7863(96)01418-7 CCC: $12.00

Chart 1. Perylene-Terminated Monodendrons

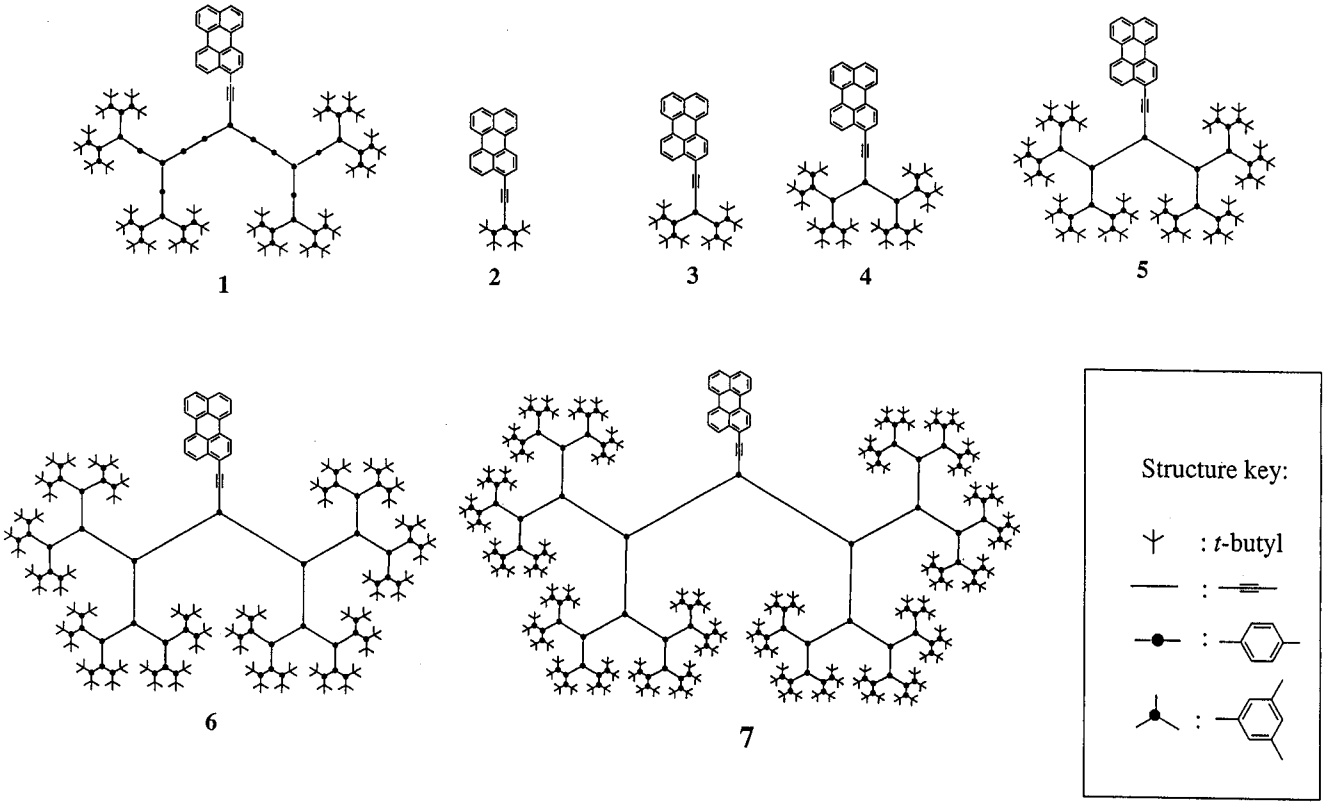

of photosynthesis.[20] Efficient photon harvesting by a multiporphyrin array with a dye molecule at one end has been reported by Lindsey and Wagner.[21] There have also been attempts to use polymeric systems with suitable chromophores to harvest solar energy radiation.[22,23] For example, Watkins and Fox reported the light-harvesting property of a well-defined block copolymer containing dimethylaniline and naphthyl or phenanthryl chromophores.[24] The energy transfer quantum yield calculated for the naphthyl system was estimated to have an upper limit of $\phi_{ET} \approx 39\%$. The assertion of polypyridine blocks as excellent molecular antennas in a polypyridine−$Ru(bpy)_2$ complex made by Yamamoto et al. is interesting.[25] However, they did not report either the energy transfer quantum yield or the energy transfer rate constant, which would give an estimate of the efficiency in that system.

Linear-chain macromolecules may not have the most ideal architecture in the design of artificial photon-harvesting systems for efficient energy transfer. Firstly, it is difficult to make polymeric systems with an energy gradient so that there can be a vectorial transduction of excitation energy. Secondly, most of the polymeric chains are flexible and therefore may form excimers which will act as an energy trap. In this regard, stiff dendritic macromolecules may be the better candidates since they have a convergent constitution which can be site specifically functionalized so that an energy gradient can exist.[26−28] Dendritic macromolecules are characterized by a large number of terminal groups originating from a focal point (core) with at least one branch at each repeat unit. We have recently reported a dendritic system from our laboratory, (**1**, Chart 1), in which the excitation energy cascades to the focal point very efficiently ($\phi_{ET} \approx 98\%$).[30,31] In **1**, the length of the linear segment between triconnected phenylacetylene moieties decreased by one unit in proceeding from the focal point to the periphery. This architecture provides an energy gradient as the energy decreases as a function of position from the periphery to the core. Hence, there is a directional energy transduction from the periphery to the core.[32]

Our motivation for this work arises, in part, from our desire to identify suitable electroactive materials for fabricating light-emitting diodes (LEDs) and highly luminescent solids for organic semiconductor lasers.[33] As a prelude to that study, the photophysical properties of various dendrimers are examined in solution and as thin solid films. In this paper, we present the energy transfer property of a series of six phenylacetylene dendrimers that uniformly vary in size and which are terminated at their focal point with the perylene luminophor. Direct excitation of phenylacetylene monodendrons results in energy transduction to perylene which serves as a reporter of energy transfer efficiency through fluoresecence. The quantum yield and rate constant of energy transfer for all six dendrimers are measured from steady-state and time-resolved fluorescence studies of the dendrimers with and without the perylene chromophores. We attempt to interpret the intramolecular

(20) Gust, D.; Moore, T. A.; Moore, A.; Devadoss, C.; Liddell, P. A.; Hermant, R. M.; Nieman, R. A.; Demanche, L. J.; DeGraziano, J. M.; Gouni, I. *J. Am. Chem. Soc.* **1994**, *116*, 9759.
(21) Wagner, S. E.; Lindsey, J. M. *J. Am. Chem. Soc*. **1994**, *116*, 9759.
(22) Webber, S. E. *Chem. Rev*. **1990**, *90*, 1469.
(23) Fox, M. A. *Acc. Chem*. Res. **1992**, *25*, 569.
(24) Watkins, D. M.; Fox, M. A. *J. Am. Chem. Soc*. **1994**, *116*, 6441.
(25) Yamamoto, T.; Yoneda, Y.; Kizu, K. *Macromol. Rapid Commun*. **1995**, *16*, 549.
(26) Tomalia, D. A.; Durst, H. D. *Top. Curr. Chem.* **1993**, *165*, 194.
(27) Frechet, J. M. J. *Science* **1994**, *263*, 1710.
(28) Xu, Z.; Kyan, B.; Moore, J. S. In *Advances in Dendritic Macromolecules*; Newkome, G. R., Ed.; Jai Press: Greenwich, CT, 1994; Vol. 1.
(29) Newkome, G. R.; Moorefield, C. N. *Adrichim. Acta* **1992**, *25*, 31.
(30) Xu, Z.; Moore, J. S. *Acta Polym*. **1994**, *45*, 83.
(31) Shortreed, M. R.; Shi, Z.-Y.; Tan, W.; Xu, Z.; Moore, J. S.; Kopelman, R. Submitted for publication.
(32) Recently, Balzani et al. have reported the synthesis of dendritic metal complexes which have photon-harvesting properties. See: Campagna, S.; Denti, G.; Serroni, S.; Ciano, M.; Juris, A.; Balzani, V. *Inorg. Chem*. **1992**, *37*, 2982.
(33) Webber, P.-W.; Liu, Y.-J.; Devadoss, C.; Bharathi, P.; Moore, J. S. *Adv. Mater*. **1996**, *8*, 237.

Chart 2. Phenyl-Terminated Monodendrons

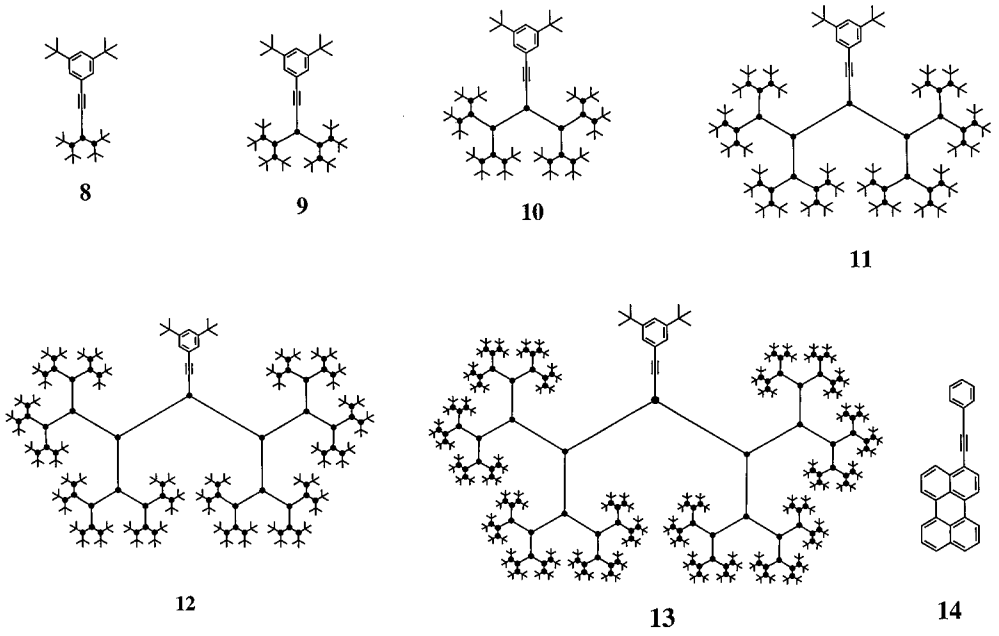

energy transfer within the context of the Förster mechanism. The energy transfer properties of this series of dendrimers are compared with those of **1**. The importance of the energy gradient in the molecule as well as the electronic coupling between different units is discussed.

Steady-State Absorption and Fluorescence Spectroscopy

The chemical structures of the perylene-terminated monodendrons are shown in Chart 1. The synthesis and characterization of these compounds are described in the Experimental Section. The structures of the reference compounds, the phenyl-terminated monodendrons, are shown in Chart 2. All these compounds have been purified by column chromatography and characterized by ^{1}H NMR, ^{13}C NMR, elemental analysis, gel permeation chromatography (GPC), high-performance liquid chromatography (HPLC), and mass spectrometry (MALDI or EI). Using HPLC, it has been possible to resolve phenyl-terminated and perylene-terminated monodendrons of the same generation, providing confirmation that perylene substitution is complete (>99.9%).

The UV−vis absorption spectra of the monodendron series **2**−**7** in dichloromethane are shown in Figure 1, and the absorption maxima (λ_{max}) and molar extinction coefficient (ϵ) are collected in Table 1. As can be seen from the spectra, there are two distinct absorption bands, one in the visible region (430−490 nm) and the other in the UV region (280−330 nm). The absorption in the visible region is due to the perylene chromophore, and that in the UV region is due to the phenylacetylene monodendrons. The absorption maximum around 260 nm also comes from the perylene chromophore. With increasing generation, the molar extinction coefficient and the position of the visible band remain constant as the inset in Figure 1 shows while the molar extinction coefficient of the UV band increases with increasing generation. Also, it should be noted that there is no spectral broadening or spectral shift with increasing generation. Only in the case of **2**, the twin peaks in the UV region lie at 290.5 and 308.0 nm whereas in all other dendrimers they lie around 293 and 310 nm, respectively. For comparison, the spectra of the reference compounds **8**−**13** (phenyl-terminated monodendrons) and **14** are shown in Figure 2, and the spectral data are summarized in Table 2. In this

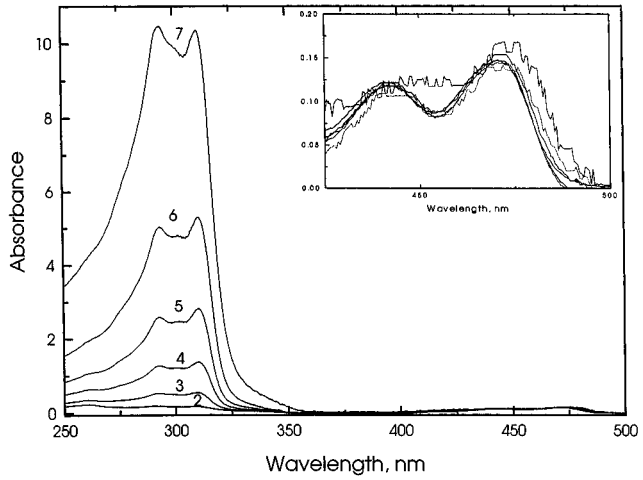

Figure 1. UV−vis absorption spectra of perylene-terminated monodendrons **2**−**7** in dichloromethane. The spectra are normalized to 3.0 μM concentration. The inset shows the expanded spectra in the region 430−500 nm.

series also, with increasing generation the intensity of absorption increases in the UV region. The very high intensity of absorption can be deduced from the large extinction coefficients of these molecules at their absorption maxima. Monodendrons **6** and **7** have especially high values of ϵ ($>1 \times 10^6$ M^{-1} cm^{-1}). One important feature of the absorption spectra is the very weak absorption of the perylene chromophore around 310 nm as can be seen from the inset in Figure 2 (reference compound **14**). This provides a window to selectively excite the monodendrons and to study the energy transfer. The absorption due to the perylene chromophore at 310 nm in the series of perylene-terminated monodendron dendrimers is 6.8% in **2**, 2.3% in **3**, and <1% in all other dendrimers.

Figure 3 shows the steady-state fluorescence spectra of perylene-terminated monodendrons **2**−**7** in dichloromethane, and the fluorescence parameters for these compounds are collected in Table 3. The samples were excited at 310 nm where most of the radiation is absorbed by the monodendrons. However, the emission is mostly from the perylene chromophore. The inset shows the residual emission from the dendrimer which is less than 5% of the perylene emission even

Table 1. Absorption Maxima and Extinction Coefficients of Perylene-Terminated Monodendrons[a]

compd	λ_{max}(abs), nm	e, M^{-1} cm^{-1}	compd	λ_{max}(abs), nm	e, M^{-1} cm^{-1}
2	470.5	4.93×10^4	**5**	471.0	5.03×10^4
	441.0	4.03×10^4		443.0	4.12×10^4
	308.0	6.07×10^4		310.5	7.97×10^5
	290.5	6.58×10^4		292.5	7.70×10^5
	260.5	8.07×10^4	**6**	472.0	4.80×10^4
3	470.5	4.83×10^4		443.0	3.93×10^4
	442.0	3.97×10^4		310.5	1.77×10^6
	310.0	1.84×10^5		293.5	1.68×10^6
	292.0	1.78×10^5	7	472.0	5.65×10^4
	260.5	1.20×10^5		445.0	4.35×10^4
4	470.5	4.93×10^4		310.5	3.45×10^6
	442.0	3.93×10^4		294.5	3.49×106
	310.0	4.57×10^5			
	293.0	4.25×10^5			

[a] All spectra were recorded in dichloromethane solution at room temperature.

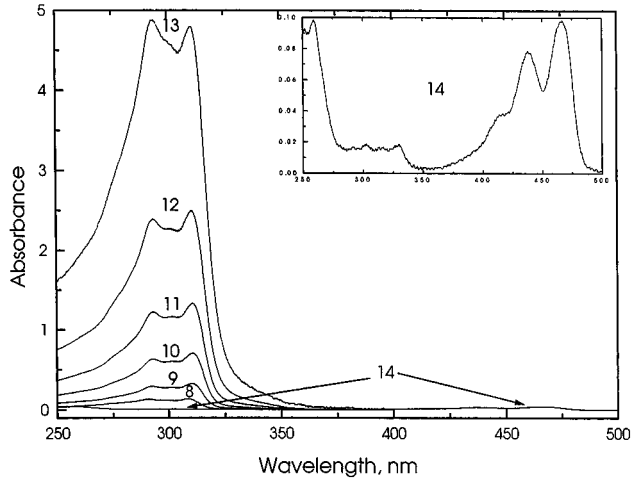

Figure 2. UV−vis absorption spectra of phenyl-terminated monodendrons **8**−**13** and the perylene derivative **14** in dichloromethane. The spectra are normalized to 1.42 μM concentration. The inset shows the absorption spectrum of **14** on an expanded scale (50×).

Table 2. Absorption Maxima and Extinction Coefficients of Phenyl-Terminated Monodendrons and Reference Compound **14**[a]

compd	λ_{max}(abs), nm	ϵ, M^{-1} cm^{-1}	compd	λ_{max}(abs), nm	ϵ, M^{-1} cm^{-1}
8	308.6	9.51×10^4	**12**	310.6	1.76×10^6
	290.0	9.15×10^4		293.4	1.68×10^6
9	310.2	2.28×10^5	**13**	311.0	3.37×10^6
	292.4	2.04×10^5		294.0	3.44×10^6
10	310.8	4.95×10^5	**14**	467.0	2.88×10^4
	293.2	4.43×10^5		437.5	2.32×10^4
11	310.8	9.38×10^5		330.0	5.59×10^3
	293.2	8.60×10^5		259.0	2.88×10^4

[a] All spectra were recorded in dichloromethane solution at room temperature.

in the higher generation (vide infra). The fact that the excitation of the phenylacetylene moiety leads to fluorescence from the perylene chromophore of the dendrimer undoubtedly indicates that intramolecular singlet−singlet energy transfer has occurred in the dendrimer. The emission spectrum of **2** is slightly blue shifted by 2 nm relative to that of other dendrimers in this series just like the absorption spectrum. The spectra of **6** and **7** are red shifted by 5 nm, and the emission spectra are also broadened. The emission spectra of the reference compounds **8**−**13** and perylene reference compound **14** are shown in Figure 4, and the data are summarized in Table 4. The phenyl-terminated monodendrons have emission maxima at ca. 360 nm with a

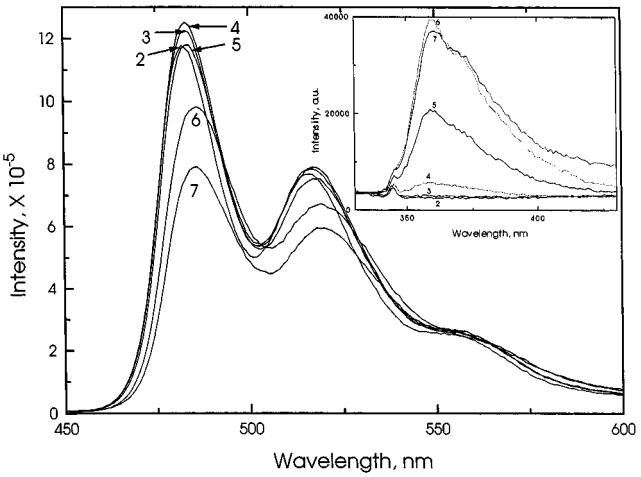

Figure 3. Steady-state fluorescence spectra (corrected) of perylene-terminated monodendrons **2**−**7** in dichloromethane. The excitation wavelength is 310 nm. The inset shows the residual fluorescence in the region 330−430 nm. All the spectra are normalized to a constant absorbance at the excitation wavelength 310 nm.

Table 3. Fluorescence Maxima, Energy Transfer Quantum Yields, and Fluorescence Lifetimes of Perylene-Terminated Monodendrons[a]

compd	λ_{max}(fl), nm	ϕ_{ET}	fluorescence lifetime, ns[b]
2	482, 515	0.95	2.3
3	483, 516	0.91	2.3
4	483, 517	0.95	2.2
5	483, 517	0.91	2.2
6	486, 519	0.85	2.4 (486 nm) (98.7%)[c] 2.5 (517 nm) (98.5%)
7	487, 519	0.54	2.3 (486 nm) (94.4%)[c] 2.4 (517 nm) (94.1%)

[a] All values are for dichloromethane solutions. The excitation wavelength is 310 nm. [b] Unless otherwise stated, decay profiles were satisfactorily fitted by a single exponential function. [c] Biexponential fit. The percentage indicates the contribution from that component.

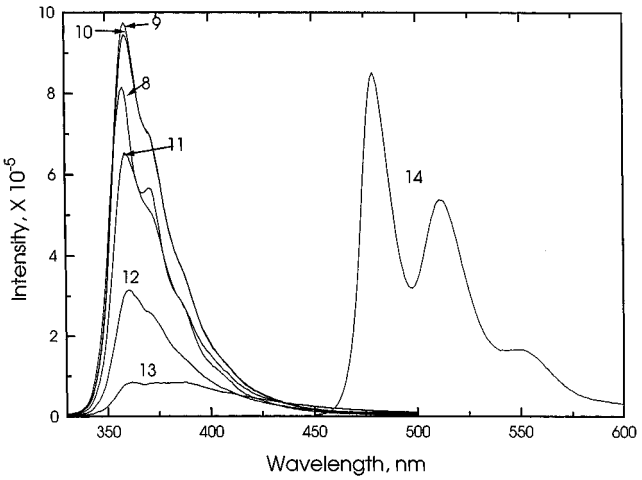

Figure 4. Steady-state fluorescence spectra (corrected) of phenyl-terminated monodendrons **8**−**13** and the perylene derivative **14** in dichloromethane. The excitation wavelength is 310 nm for **8**−**13** and 440 nm for **14**. All the spectra (except that of **14**) are normalized to a constant absorbance at the excitation wavelength 310 nm.

shoulder at ca. 370 nm. The perylene reference compound **14** has emission maxima at 479 and 512 nm. The emission from perylene-terminated monodendrons is slightly red shifted by about 4 nm, which is the same shift observed in the absorption spectra.

As the inset in Figure 3 indicates, in the higher generation monodendrons there is a residual fluorescence in the range 330−430 nm from the phenylacetylene moiety. The fluorescence

Table 4. Fluorescence Maxima, Quantum Yields, and Lifetimes of Phenyl-Terminated Monodendrons and Reference Compound **14**[a]

compd	λ_{max}(fl), nm	ϕ_{fl}	lifetime, ns[b]
8	358, 371 (sh)	0.26	8.4
9	359, (372)	0.31	7.6
10	359, 374	0.31	3.7
11	361, 372	0.23	3.2
12	360, 374	0.12	2.5 (80%)[c]
13	365, 390	0.06	0.68 (70.4%)[c]
14	479, 512		2.3

[a] All values are for dichloromethane solutions. The excitation wavelength is 310 nm except for **14**, which was excited at 440 nm (steady state) and 467 nm (lifetime measurement). [b] Unless otherwise stated, decay profiles were satisfactorily fitted by a single exponential function. [c] Bioexponential fit. The percentage indicate the contribution from that component.

quantum yields (ϕ_{fl}) of perylene-terminated monodendrons follow the order **3** > **4** > **2** > **5** > **6** > **7**, and those of phenyl-terminated monodendrons follow the order **10** > **9** > **8** > **11** > **12** > **13**. Clearly, the higher generation dendrimers have lower ϕ_{fl} values. For perylene-terminated dendrimers, the trend in ϕ_{fl} in the region 330−430 nm is reversed. The higher generation dendrimers have larger residual fluorescence. This indicates that the efficiency of energy transfer (ϕ_{ET}) decreases with increasing generation. The efficiency of energy transfer is the measure of the probability that a localized excitation on a monodendron is transmitted to the perylene chromophore at the focal point.

The effect of solvent polarity on the spectral characteristics of the perylene-terminated monodendrons was examined by recording the absorption and fluorescence spectra of **4** in cyclohexane (CHX), dichloromethane (DCM), and tetrahydrofuran (THF). Interestingly, only the visible band (due to the perylene chromophore) is affected, and the absorption due to the phenylacetylene segments remains unchanged. In CHX, the absorption maximum is blue shifted by about 5 nm and the fluorescence spectrum by 6 nm from those in THF and DCM. The absorption and emission spectra of **14** were also recorded in those three solvents. As expected, the absorption maximum and the fluorescence maximum in CHX are blue shifted by about 5 and by 4 nm, respectively, from the values in DCM.

To study the effect of generation on the photon-harvesting ability of the dendrimers, the excitation spectra of the perylene-terminated monodendrons were recorded by monitoring the emission at 515 nm, and the spectra were normalized to a constant intensity value at 470 nm, where the perylene chromophore alone absorbs. These spectra are shown in Figure 5. As can clearly be seen from the region around 310 nm, which is the characteristic feature of the absorption due to phenyacetylene moieties, with increasing generation more photons are collected and transmitted to perylene. There is a monotonic increase in photon-harvesting efficiency with increasing generation, and even the highest generation dendrimer shows no sign of reaching an asymptotic limit in excitation intensity. Therefore, higher generation dendrimers with a large number of phenylacetylene groups will serve as better antennas.

Time-Resolved Fluorescence Spectroscopy

The fluorescence lifetimes of the perylene-terminated monodendrons and the reference compounds were measured in dichloromethane solution using a time-correlated single photon counting (TCSPC) instrument. The samples were excited at 310 nm except for **14**, which was excited at 467 nm. The fluorescence decay was monitored at the emission peak, and in the case of perylene-terminated monodendrons fluorescence decay was monitored at both maxima in the emission band. As an example of typical data, the fluorescence decay of **5** monitored at 359 nm is shown in Figure 6 with the excitation lamp profile and the fitted curve. The fluorescence trace was well-fitted by a monoexponential decay function, and the lifetime of the monodendron is 3.2 ns. The values of the fluorescence lifetime are given in Tables 3 and 4. As can be inferred from these data, the lifetimes of the reference monodendrons decrease with increasing generation. This same trend was also observed in the fluorescence quantum yields. This behavior indicates that in higher generations there is a competing nonradiative process. One possibility is fast intersystem crossing to form dendrimer triplets. No experiments have been done to verify this hypothesis. At this juncture, it is important to point

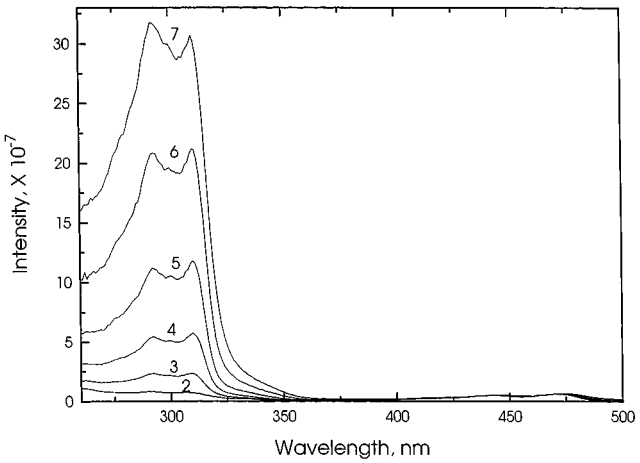

Figure 5. Excitation spectra of perylene-terminated monodendrons **2**−**7** in dichloromethane. The monitoring wavelength is 515 nm. The spectra have been normalized to a constant intensity at 470 nm.

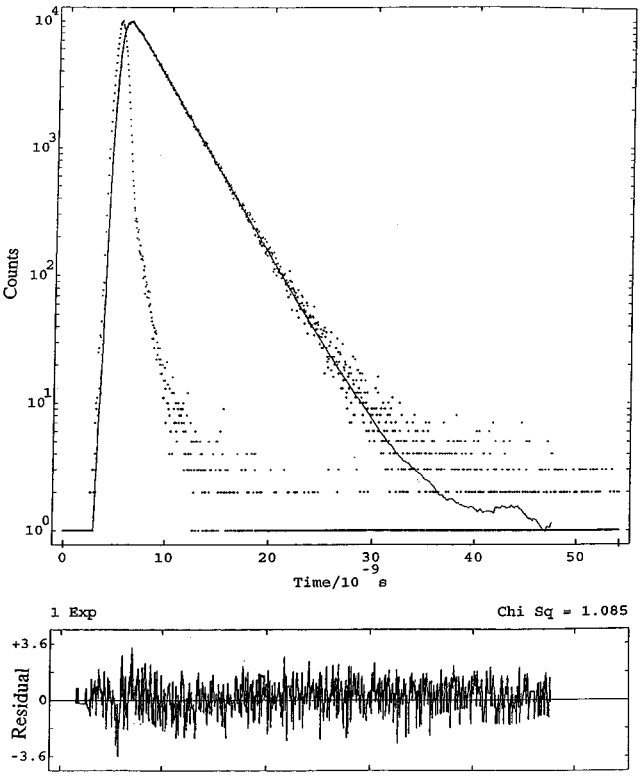

Figure 6. Fluorescence decay curve for the monodendron **11** in dichloromethane. The excitation wavelength is 310 nm, and the monitoring wavelength is 359 nm. The sharp decay curve is the lamp profile, and the solid line is the fitted curve. The fluorescence profile was fitted to a monoexponential decay with a lifetime of 3.2 ns. The bottom trace shows the weighted residuals distribution for the monoexponential fit ($\chi^2 = 1.085$).

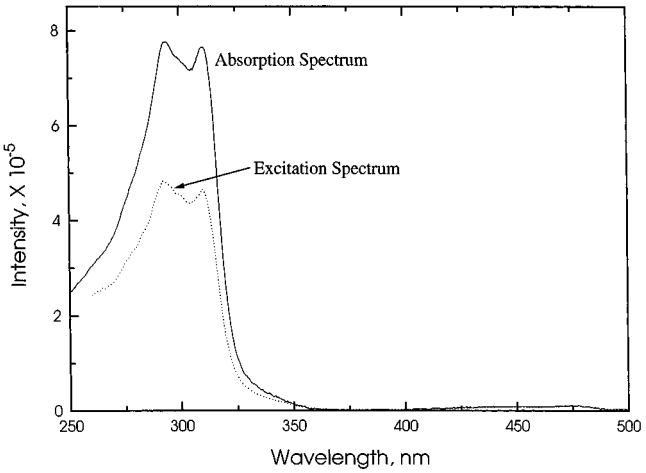

Figure 7. Absorption (solid line) and corrected excitation (dashed line) spectra of the monodendron **7** in dichloromethane. The spectra were normalized at the perylene absorption region (430−500 nm).

out that the analogous compound tolan (diphenylacetylene) has a fluorescence lifetime of about 200 ps.[34]

The lifetimes of perylene-terminated dendrimers are all the same (∼2.3 ns), which are obtained by monitoring the emission at 485 and 515 nm. This constant value is expected as the fluorescence emanates from the perylene chromophore. The fluorescence lifetime of the reference compound **14** is also 2.3 ns. We were unable to measure the lifetime of perylene-terminated monodendrons in the emission band of the phenylacetylene wedges (around 360 nm). The residual emission was too weak to measure with our instrument.

Excitation Energy Transfer

The singlet−singlet energy transfer in the perylene-terminated monodendrons from the phenylacetylene moieties to the perylene chromophore can be studied quantitatively using steady-state fluorescence excitation spectroscopy. The energy transfer quantum yield can be estimated by comparing the absorption spectrum and excitation spectrum of perylene-terminated monodendrons by monitoring the emission of the acceptor, i.e., perylene.[20,35] For example, Figure 7 shows the corrected excitation spectrum of **7** which has been multiplied by a factor to normalize to the absorption spectrum of **7** in the 460−480 nm range where the phenylacetylene monodendrons do not absorb appreciably. It is clear from the figure that, in regions where the monodendrons absorb (280−320 nm), the characteristic features of the absorption spectrum of the reference compound are evident although their intensities are different. In the case of total energy transfer, i.e., $\phi_{ET} = 1$, the band shape and intensity of those spectra would be identical. The singlet−singlet energy transfer efficiency for **7** is ∼54%, as estimated from the ratio of the normalized corrected excitation spectrum and absorption spectrum at 310 nm (i.e., the absorption maximum of phenylacetylene monodendrons). The experiment is valid if we assume that ϕ_{fl} for perylene is independent of the mode of excitation (by either direct irradiation or energy transfer). This assumption is valid since the fluorescence lifetime of the perylene chromophore is independent of generation and is identical to that of the reference compound **14**. Similar experiments were carried out for other perylene-terminated monodendrons. The values of ϕ_{ET} for the entire

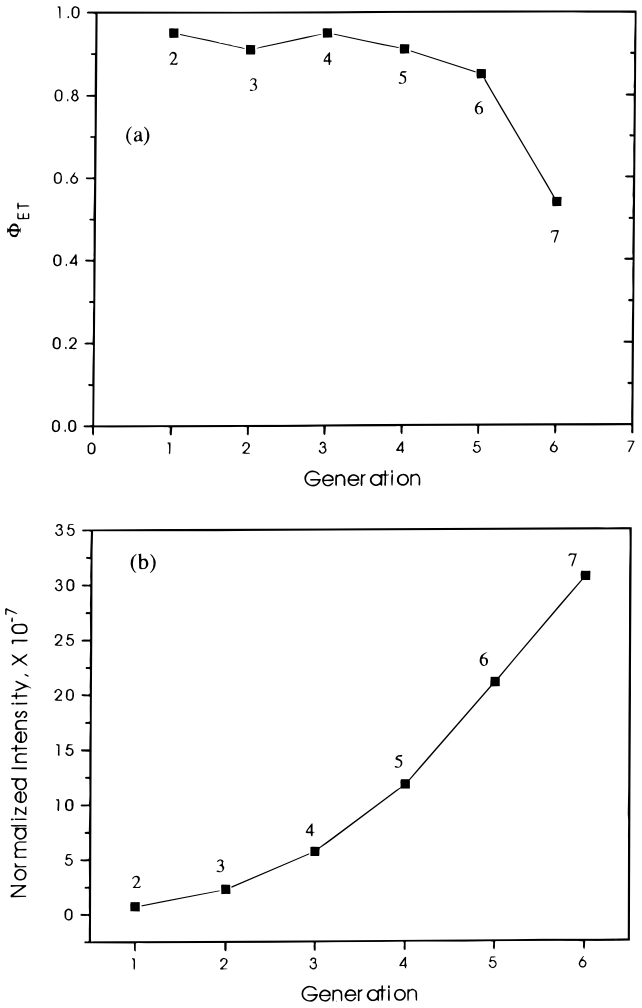

Figure 8. (a) Quantum yield of energy transfer in the monodendrons **2**−**7** as a function of generation. (b) Intensity at 310 nm of the normalized excitation spectra of perylene-terminated monodendrons **2**−**7** in dichloromethane as a function of generation.

series of dendrimers are given in Table 3. From the value of ϕ_{ET} and the lifetime of the corresponding phenyl-terminated monodendrons, the rate constant for energy transfer (k_{ET}) can be calculated using the following equation:

$$k_{ET} = \frac{1}{\tau_D}\left(\frac{1}{(1/\phi_{ET}) - 1}\right) \quad (1)$$

where τ_D is the lifetime of the dendrimer fluorescence in the absence of the acceptor (i.e., the lifetime of the corresponding phenyl-terminated monodendrons) and ϕ_{ET} is the energy transfer efficiency. The relationship between the ϕ_{ET} and the generation of the dendrimers is depicted in Figure 8a. The energy transfer efficiency decreases significantly in the higher generation of dendrimers. This trend can be ascribed, in the context of the Förster mechanism of energy transfer, to the influence of the distance between the donor and the acceptor, the overlap integral between the phenylacetylene monodendrons and the perylene chromophore, and the radiative constants of the donors.

Energy Transfer in 1: A Monodendron with an Energy Gradient

Compound **1**, unlike perylene-terminated monodendrons **2**−**7**, consists of triconnected phenylacetylene monomers augmented with linear segments of phenylacetylene moieties.[31] These linearly connected segments form localized regions of extended π-conjugation. The length of the linear segments between the

(34) Hirata, Y.; Okada, T.; Mataga, N.; Nomoto, T. *J. Phys. Chem.* **1992**, *96*, 6559.

(35) Schulman, S. G. *Molecular Luminescence Spectroscopy: Methods and Applications*; John Wiley & Sons, Inc: New York, 1993; Vol. 3.

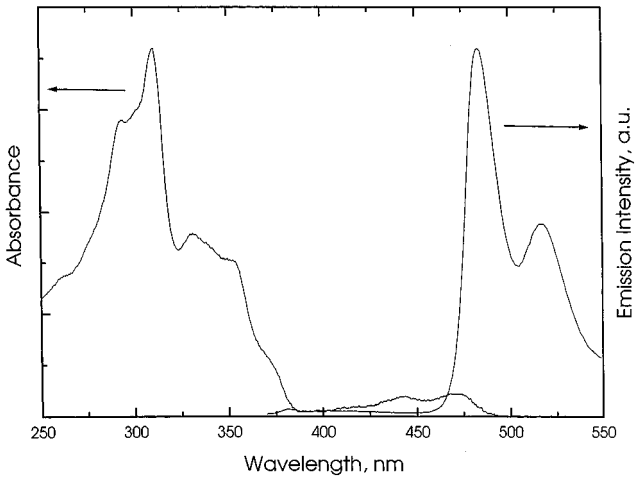

Figure 9. Absorption and fluorescence spectra of the perylene derivative **1** in dichloromethane. The excitation wavelength is 310 nm, and the monitoring wavelength is 515 nm.

triconnected junctures is decreased by one unit in proceeding from the core to the rim. By controlling the spatial location of these moieties, thereby the energy levels of the localized electronic states, energy as a function of position decreases smoothly from the periphery to the core. This creates an energy gradient which results in a directional energy flow. This is reflected in the absorption spectrum of **1**, which has an additional band besides those observed for other monodendrons with λ_{max} at 331 nm and a shoulder at 354 nm (Figure 9). Unlike the absorption spectrum, the steady-state fluorescence spectrum of **1** is similar to that of other monodendrons. When **1** is excited at 310 nm where the phenylacetylene chromophore absorbs, the emission occurs from the perylene chromophore with emission peaks at 484 and 518 nm (Figure 9). The residual fluorescence from the phenylacetylene monodendron in the range 340−420 nm is very weak. By comparing the absorption and fluorescence excitation spectra of **1**, the quantum yield of energy transfer in **1** was estimated to be 98%. The fluorescence lifetime of the reference compound for **1** was measured to be 270 ps.[36] From these values the rate constant for energy transfer, k_{ET}, was calculated to be 1.9×10^{11} s^{-1}. Hence, in **1** the intramolecular energy transfer occurs at a very fast rate relative to **6**, a dendrimer of comparable size. This fast rate can be ascribed to the directional flow of excitation energy as well as the electronic coupling of the different phenylacetylene moieties. It should also be pointed out that in **1** there is a larger overlap between the emission of the donor and the absorption of the acceptor.

Excitation Energy Transfer Mechanism

The inter- and intramolecular electronic excitation energy transfer can occur nonradiatively through either Coulombic interaction (Förster mechanism) or exchange interaction (Dexter mechanism).[20,37,38] In the Dexter mechanism, the exchange interaction is a quantum mechanical effect arising from the symmetry properties of the wave functions with regard to the exchange of the space and spin coordinates of electrons in the donor−acceptor system. The Dexter mechanism requires the spatial overlap of the orbitals of the donor and the acceptor. This interaction is necessarily of short range, and it falls-off exponentially. In general, the Dexter mechanism is invoked to explain triplet−triplet energy transfer. Most of the experimental observations of singlet−singlet energy transfer are interpreted in terms of the Förster mechanism. Basically, the Förster mechanism operates through the Coulombic interactions between the donor and the acceptor transition dipoles. Resonant coupling of the donor "transmitter" and acceptor "receiver" leads to energy transfer. Förster's relation for long-distance dipole−dipole energy transfer is given by

$$k_{ET} = \frac{9000(\ln 10)\kappa^2\phi_D J}{128\pi^5 n^4 N \tau_D R^6} \qquad (2)$$

In eq 2, κ^2 is a function of the relative orientation of the transition dipole moments (vide infra), ϕ_D and τ_D are the fluorescence quantum yield and the excited singlet state lifetime of the donor in the absence of the acceptor, J is the overlap integral, n is the index of refraction of the solvent (CH_2Cl_2), N is the Avogadro's number, and R is the distance between the centers of the two dipoles (cm).

The overlap integral J (cm^6/mol) is given by the equation

$$J = \int f_D(\nu)\, \epsilon_A(\nu)\, \nu^{-4}\, d\nu \qquad (3)$$

where $f_D(\nu)$ is the fluorescence spectrum of the donor normalized on the wavenumber scale (ν) and $\epsilon_A(\nu)$ is the molar extinction coefficient of the acceptor at that wavenumber. The integral J, which represents the overlap of the donor emission spectrum and the acceptor absorption spectrum, is one of the deciding factors which affect the rate of energy transfer. The orientation factor κ^2 depends on the angle between the transition dipoles and is given by

$$\kappa^2 = (\cos\gamma - 3\cos\alpha\cos\beta)^2 \qquad (4)$$

where α and β are angles which the transition dipoles make with the line joining the centers of the dipoles and γ is the angle between the two transition dipoles. κ^2 can have values in the range between 0 and 4.

Attempts to apply the Förster mechanism to this system are fraught with difficulty. It is not certain whether the energy transfer occurs in one hop or through a multistep hopping pathway. In the case of perylene-terminated monodendrons, the distance R is not obvious. Using molecular models, we estimate this distance as the separation between the center of the middle ring of the perylene chromophore (acceptor) and the carbon atom of the farthest acetylenic bond. Therefore, the dendrimers **2**−**7** have 2, 4, 8, 16, 32, and 64 values for R, respectively. The approximation that only the peripheral phenylacetylene moieties are considered for energy transfer calculation is based on the fact that there are more chromophores in the periphery than anywhere else in the molecule. The orientations of the transition dipoles of the donor and the acceptor moieties is assumed to be random in all the dendrimers under study, and a value of 2/3 is assigned to κ^2. This approximation is justifiable especially in the higher generations as the orientation of the phenylacetylene moieties around the perylene chromophore approaches a random distribution. The overlap integrals for the perylene-terminated dendrimers were calculated using the fluorescence spectra of the corresponding phenyl-terminated dendrimer and the absorption spectrum of the reference compound **14**. For every perylene-terminated

(36) The reference compound chosen for **1** is the corresponding iodo-terminated monodendron. Even though it is not the ideal choice because of its expected heavy atom effect, it is justified since a similar lifetime has been observed for the ethynyltrimethylsilyl-terminated monodendron (τ = 500 ps, ref 31). Further, the fluorescence quantum yield of the reference compound is high (ϕ_{fl} = 0.74), suggesting a weak heavy atom effect.

(37) Lamola, A. A.; Turro, N. J. *Energy Transfer and Organic Photochemistry*; Interscience Publishers: New York, 1969.

(38) van Grondelle, R. *Biochim. Biophys. Acta* **1985**, *811*, 147.

Table 5. Overlap Integral (J), Critical Transfer Distance (R_0) and Calculated and Observed Energy Transfer Rate Constants for the Perylene-Terminated Monodendrons

compd	J, mol^{-1} cm^6	R_0, Å[a]	calcd k_{ET}, s^{-1} [b]	obsd k_{ET}, s^{-1}
2	7.03×10^{-15}	25.3	7.75×10^9	2.26×10^9
3	7.65×10^{-15}	26.4	2.66×10^9	1.34×10^9
4	7.81×10^{-15}	26.5	2.63×10^9	5.13×10^9
5	9.06×10^{-15}	25.8	1.45×10^9	3.21×10^9
6	1.18×10^{-14}	24.2	4.67×10^9	2.27×10^9
7	2.46×10^{-14}	24.4	3.14×10^{10}	1.75×10^9

[a] $R_0 = 9000(\ln 10)\kappa^2\phi_D J/128\pi^5 n^4 N$. [b] $k_{ET}(\text{calcd}) = (1/\tau_D)[R_0/R]^6$. κ^2 was assumed to be 0.667 for all dendrimers.

dendrimer under study, the energy transfer rate constant was calculated for each R value and then the average value of the rate constant was obtained. The calculated overlap integral J, the critical transfer radius R_0, the average of the calculated energy transfer rate constants, and the experimental rate constants are collected in Table 5. As can be seen from the table, there is a lack of complete correlation between the calculated rate constants and the experimental values. Clearly, this simplistic attempt to apply the Förster mechanism fails to explain the intramolecular electronic energy transfer in these dendrimers. Results do not suggest that a significant amount of excitation occurs from the dendrimer interior and not the periphery groups. Perhaps they imply a multistep process.

Discussion

The perylene-terminated dendrimers possess a globular, macromolecular architecture which exhibits efficient intramolecular excitation energy transfer. Dendrimers have a spatially controlled structure which can be site-specifically functionalized. Moreover, in sharp contrast to linear polymers which can assume conformations from an extended chain to a compact coil depending on the solvent and temperature, dendrimers presumably have consistent globular shape in solution. Since dendrimers are prepared by iterative stepwise processes, the problem of polydispersity is significantly reduced unlike in the linear polymers.

As can be seen from the excitation spectra (Figure 8b), these dendrimers are very good light-harvesting agents. The light-gathering "antenna" property increases with increasing generation. With increasing size, the number of light-absorbing phenylacetylene chromophores increases, making the higher generation dendrimers better photon-harvesting agents. However, the efficiency of energy transfer to the core decreases with increasing generation (Figure 8a). The photoluminescence intensity from the perylene core depends on the extinction coefficient (ϵ) of the donor monodendron and the efficiency of energy transfer, ϕ_{ET}. Therefore, there is a trade-off between increasing ϵ with increasing generation and the corresponding decreasing ϕ_{ET}. We anticipate that as the dendrimer becomes larger the photoluminescence intensity will decrease or level off with increasing size of the dendrimer. However, we have not reached that stage yet. As the generation increases, nonradiative processes may intervene, dissipating the excitation energy. This is evident from the decreasing fluorescence quantum yield with increasing generation. Larger dendrimers can provide more channels for the dissipation of excitation energy and have a greater average distance from the peripheral groups to the core.

Dendrimer **1** has a significantly faster rate (by 2 orders of magnitude) of energy transfer relative to **2**−**7**. The main difference between **1** and **2**−**7** is the electronic energy gradient, from the periphery to the core built into dendrimer **1**. This gradient apparently facilitates the directional transduction of excitation energy to the focal point. In the dendrimers **2**−**7**, the electronic coupling between phenylacetylene chromophores is weak since they are cross conjugated through meta aromatic linkages. To explain the fast rate of energy transfer in **1**, we have considered the increase in overlap between the emission spectrum of the donor and the absorption of the acceptor. However, calculations of the overlap integral for **1** vs **2**−**7** cannot alone account for the 10^2 rate increase. An alternate explanation may be related to the unique topology of the dendrimer structure. Beratran et al. have considered regular dendrimers as Bethe lattices, a special class of ordered fractals with electronic properties different from those of small molecules and 1-D polymers.[39] Kopelman et al. have described the unique features that the fractal structure contributes to energy transfer efficiency.[31] They considered electronic excitation energy to be localized within each segment with only weak coupling between adjacent segments.

The lack of perfect correlation between the predicted and observed energy transfer rate constants for the series of dendrimers under study is not surprising when one considers the many factors which change with generation. This includes the distribution of interchromophore distances, the overlap integral, the fluorescence quantum yield, and the fluorescence lifetime of the donor in the absence of the acceptor. An important aspect in this system is that the interchromophore distance is not single valued but is better described by a distribution. Because of the dependence on multivariables, the system is not amenable to simple interpretation by the Förster mechanism. A similar observation was noted in the array of porphyrins reported by Lindsey and Wagner.[21]

The photophysical study of these dendrimers in the solid state and their suitability for LEDs is underway in our laboratory. These dendrimers, especially the higher generation ones, have very high molar extinction coefficients, and hence they can be used as sensors for trace elements with suitable ligands. They are also good systems for a two-photon spectroscopic study.

Conclusions

We have synthesized and characterized the perylene-terminated dendrimers **2**−**7** and phenyl-terminated reference dendrimers **8**−**14**. The intramolecular energy transfer in **1**−**7** has been studied using steady-state as well as time-resolved fluorescence spectroscopy. In the series **2**−**7**, the light-harvesting ability of these compounds increases with increasing generation. With increasing number of phenylacetylene moieties the number of energy-collecting sites increases, and hence they are efficient light harvesters. However, the efficiency of the energy transfer decreases with increasing generation in this series. With increasing generation the photoluminescence intensity increases and the expected level-off has not yet been reached. Dendrimer **1** is unique in that energy transfer occurs at a very fast rate. This ultrafast energy transfer has been attributed to the energy gradient from the periphery to the focal point in **1**. The energy transfer process could not be explained by the Förster mechanism.

Experimental Section

(a) Spectroscopic Measurements. The UV−vis absorption spectra were recorded on a Shimadzu (model UV-160A) spectrophotometer using 1-cm quartz cells. Fluorescence spectra were recorded on a Photon Technology International (PTI) QM-1 fluorometer. The optical density of the solution for fluorescence measurements was less than 0.1 at the excitation wavelength. The fluorescence quantum yields of

(39) Risser, S. M.; Beratan, D. N.; Onuchic, J. N. *J. Phys. Chem.* **1993**, *97*, 4523.

the samples were determined against quinine sulfate solution in 0.1 N H_2SO_4 ($\phi_{fl} = 0.55$) as the standard.[40] Fluorescence and excitation spectra were corrected for the wavelength dependence of detector sensitivity and excitation light source output. The spectra were recorded using a 1-cm quartz cuvette in the right angle geometry at room temperature.

Fluorescence lifetimes were measured on a time-correlated single photon counting fluorometer (Edinburgh Instruments, model OB9000). The excitation source was a coaxial hydrogen flash lamp operated at 40 kHz. The emission was detected at a right angle to the excitation light with a Hamamatsu R955 photomultiplier tube (PMT) which was cooled to −22 °C. The response time of the PMT was 2.2 ns. A total of 10 000 counts were collected in the maximum channel. The absorbance of the solutions was between 0.2 and 0.5 at the excitation wavelength. The fluorescence decay profile was analyzed by reconvolution of the instrumental response function and monoexponential or multiexponential decay of the emission using an iterative nonlinear least squares method. The goodness-of fit was assessed by using the plots of weighted residuals, reduced χ^2 values, and Durbin−Watson (DW) parameters.

(b) Synthesis. Unless otherwise indicated, all starting materials were obtained from commercial suppliers (Aldrich, Lancaster, Fischer, Mallincrodt, J. T. Baker, EM Science) and were used without purification. Hexane, dichloromethane, and ethyl acetate were distilled before use. All atmosphere sensitive reactions were done under nitrogen using a vacuum line or in a drybox. Analytical TLC was performed on KIESELGEL F-254 precoated silica gel plates. Visualization was accomplished with UV light or phosphomolybdic acid stain. Flash chromatography was carried out with Silica Gel 60 (230−400 mesh) from EM Science. Dry triethylamine was obtained by vacuum transfer from calcium hydride. Dry THF was obtained by vacuum transfer from sodium and benzophenone.

^{1}H and ^{13}C NMR spectra were recorded on a Bruker AM-360, Varian Unity 400, or Varian XL-200 spectrometer. Chemical shifts were recorded in parts per million (δ), and splitting patterns are designated as s (singlet), d (doublet), t (triplet), q (quartet), m (multiplet), and br (broad). Coupling constants, *J*, are reported in hertz (Hz). The residual proton signal of the solvent was used as an internal standard for spectra recorded in chloroform-*d* (δ 7.26 for ^{1}H, δ 77.0 for ^{13}C), benzene-d_6 (δ 7.15 for ^{1}H, δ 128 for ^{13}C), Gas chromatography (GC) was performed on a HP-5890 Series II gas chromatograph equipped with a 12.5m × 0.2 mm × 0.5 μm HP-1 methyl silicone column and fitted with a flame ionization detector and helium carrier gas at 30 mL/min. Low-resolution mass spectra were obtained on either a Hewlett-Packard GC−MS equipped with a 30 m HP-1 capillary column operating at 70 eV or a Finnigan-MAT CH5 spectrometer operating at 70 eV. High-resolution electron impact mass spectra were obtained on a Finnigan-MAT 731 spectrometer operating at 70 eV. Low- and high-resolution fast atom bombardment (FAB) mass spectra were obtained on VG ZAB-SE and VG 70-SE-4F spectrometers. Elemental analyses were performed by the University of Illinois Microanalytical Service Laboratory using a Leeman Labs CE440. Analytical HPLC was performed with a Rainin Dyanamax solvent delivery system, model SD-200, using a Microsorb Si-80-125-C5 silica column. GPC was performed using a Waters 510 HPLC pump, Waters 996 photodiode array detector, and a series of three Waters styragel HR 4E 7.8 × 300 mm columns which were calibrated with narrow molecular weight polystyrene standards. GPC data were obtained in THF at 35 °C.

(3,5-Di-*tert*-butylphenyl)acetylene and the precursor monodendrons (iodo-terminated) were prepared by a previously reported procedure.[41] The synthesis of **1** has been previously reported.[30] 3-Acetylperylene was prepared according to the procedure reported in the literature.[42]

3-Ethynylperylene. The procedure for the conversion of 3-acetylperylene to 3-ethynylperylene was adopted from the literature.[43] A three-necked round-bottomed flask was charged with tetrahydrofuran (THF) (10 mL) under nitrogen. To this was added sequentially at 0 °C diisopropylamine (1.1 mmol) and *n*-butyllithium in hexane (1.1 mmol). The reaction mixture was stirred for 30 min and cooled to −78 °C. 3-Acetylperylene (1 mmol) dissolved in hot THF (60 mL) was cooled and slowly added. After the mixture was stirred for 1 h at −78 °C, diethyl chlorophosphate (1 mmol) was added, and the reaction mixture was allowed to warm to room temperature over 3 h. A second lot of lithium diisopropylamide (2.5 mmol) in THF was prepared in another flask and cooled to −78 °C. To this was added slowly with a double-ended needle under nitrogen the above prepared reaction mixture. The resulting solution was allowed to warm to room temperature. After being stirred for 12 h it was quenched with water (20 mL) and extracted with dichloromethane (3 × 20 mL). The combined organic layer was treated with cold hydrochloric acid (1 N, 50 mL), water (2 × 20 mL), and saturated sodium bicarbonate solution (20 mL), dried over sodium sulfate, and evaporated. The dark yellow solid obtained was purified by column chromatography (3% CH_2Cl_2/hexane) to obtain a 47% yield of pure 3-ethynylperylene. The purity of the compound was determined by analytical HPLC. ^{1}H NMR (400 MHz, $CDCl_3$) δ 8.25−8.13 (m, 4H), 8.10 (d, $J = 8$ Hz, 1H), 7.72−7.64 (m, 3H), 7.55 (t, $J = 8$ Hz, 1H), 7.47 (dt, $J = 8$, 1.7 Hz, 2H), 3.55 (s, 1H). ^{13}C NMR (100 MHz, $CDCl_3$) δ 134.85, 134.51, 132.26, 131.77, 131.42, 130.83, 130.48, 128.49, 128.35, 128.06, 127.34, 126.62, 125.89, 121.02, 120.67, 119.35, 118.94, 82.82, 82.14. MS (EI) calcd for $C_{22}H_{12}$ 276.3, found 276.

General Procedure for the Pd(0)-Catalyzed Coupling of Monodendrons with 3-Ethynylperylene. A heavy-walled flask was charged with 3-ethynylperylene (1.2 equiv), iodo-terminated monodendron **I-M$_y$-(*t*-Bu)$_x$** (1.0 equiv), $Pd(dba)_2$ (0.02 equiv), triphenylphosphine (0.10 equiv), copper(I) iodide (0.02 equiv), and triethylamine. The concentration of the reaction varied from 0.3 to 0.05 M depending on the solubility of reactants and the scale of the reaction. The flask was then evacuated and back-filled with nitrogen three times, sealed, and stirred at 50 °C for 12 h or until the reaction was complete. The disappearance of **I-M$_y$-(*t*-Bu)$_x$** was monitored by TLC. When the reaction was finished, the mixture was filtered, the filter cake was washed with hexane, and the combined filtrates were evaporated to dryness. The product was purified as outlined below.

14. 3-Ethynylperylene and iodobenzene were reacted using the general coupling procedure, and the product was purified by column chromatography eluting with hexane to 2% CH_2Cl_2/hexane. Yield 60%. ^{1}H NMR (400 MHz, $CDCl_3$) δ 8.29 (d, $J = 8.3$ Hz, 1H), 8.24 (d, $J = 8.3$ Hz, 1H), 8.19 (d, $J = 8.4$ Hz, 2H), 8.14 (d, $J = 8$ Hz, 1H), 7.73 (d, $J = 7.5$ Hz, 1H), 7.68 (dd, $J = 3$, 8 Hz, 2H), 7.64 (d, $J = 6.5$ Hz, 2H), 7.58 (t, $J = 8$ Hz, 1H), 7.48 (t, $J = 8$ Hz, 2H), 7.43−7.33 (m, 3H). ^{13}C NMR (100 MHz, $CDCl_3$) δ 134.61, 131.62, 131.01, 128.54, 128.45, 128.40, 128.38, 128.06, 127.25, 126.67, 126.60, 123.36, 88.02, 86.68. MS (FAB) calcd for $C_{28}H_{16}$ 352.4, found 352.1.

2. 3-Ethynylperylene and **I-M$_3$-(*t*-Bu)$_4$** were reacted using the general coupling procedure, and the product was purified by column chromatography eluting with hexane to 4% CH_2Cl_2/hexane.[41] Yield 55%. ^{1}H NMR (400 MHz, $CDCl_3$) δ 8.36−8.13 (m, 5H), 7.84−7.68 (m, 6H), 7.63 (t, $J = 8$ Hz, 1H), 7.51 (t, $J = 8$ Hz, 2H), 7.45−7.41 (m, 6H), 1.35 (s, 36H). ^{13}C NMR (100 MHz, $CDCl_3$) δ 150.92, 134.55, 133.76, 132.07, 131.46, 131.18, 130.91, 130.61, 128.45, 128.40, 128.07, 127.32, 126.64, 126.55, 125.97, 124.30, 124.03, 123.12, 121.74, 119.70, 93.91, 91.71, 89.08, 86.71, 34.84, 31.33. MS (FAB) calcd for $C_{60}H_{56}$ 777.1, found 776.4.

3. 3-Ethynylperylene and **I-M$_7$-(*t*-Bu)$_8$** were reacted using the general coupling procedure, and the product was purified by column chromatography eluting with 3% CH_2Cl_2/hexane to 8% CH_2Cl_2/hexane.[41] Yield 92%. ^{1}H NMR (400 MHz, $CDCl_3$) δ 8.34−8.12 (m, 5H), 7.82−7.57 (m, 13H), 7.49 (t, $J = 8$ Hz, 2H), 7.45−7.32 (m, 12H), 1.35 (s, 72H). ^{13}C NMR (100 MHz, $CDCl_3$) δ 150.92, 134.57, 134.45, 134.30, 134.17, 133.93, 132.25, 131.53, 131.35, 130.93, 130.62, 128.51, 128.43, 128.12, 127.43, 126.69, 126.60, 125.97, 124.34, 123.79, 123.35, 123.14, 121.71, 119.65, 119.57, 93.60, 91.77, 89.51, 89.28, 88.64, 86.59, 34.84, 31.33. MS (FAB) calcd for $C_{108}H_{104}$ 1401.9, found 1401.9.

4. 3-Ethynylperylene and **I-M$_{15}$-(*t*-Bu)$_{16}$** were reacted using the general coupling procedure, and the product was purified by column chromatography eluting with 5% CH_2Cl_2/hexane to 10% CH_2Cl_2/hexane.[41] Yield 92%. ^{1}H NMR (400 MHz, $CDCl_3$) δ 8.34−8.12 (m, 5H), 7.82 (d, $J = 1.5$ Hz, 2H), 7.79−7.56 (m, 23H), 7.49 (t, $J = 8$ Hz, 2H), 7.45−7.34 (m, 24H), 1.34 (s, 144H). ^{13}C NMR (100 MHz, $CDCl_3$) δ 150.91, 134.62, 134.59, 134.45, 133.92, 125.96, 124.34, 123.85,

(40) Demas, J. N.; Crosby, J. A. *J. Phys. Chem.* **1971**, *75*, 991.
(41) Bharathi, P.; Patel, U.; Kawaguchi, T.; Pesak, D. J.; Moore, J. S. *Macromolecules* **1995**, *28*, 5955.
(42) Zeiger, H. E. *J. Org. Chem.* **1966**, *31*, 1977.
(43) Negishi, E.; King, A. O.; Tour, J. M. *Org. Synth.* **1985**, *64*, 44.

123.72, 123.67, 123.31, 123.13, 121.69, 91.79, 89.38, 88.94, 88.5, 86.56, 34.83, 31.32. MS (MALDI) calcd for $C_{204}H_{200}$ 2652, found 2652. Anal. Calcd for $C_{204}H_{200}$: C, 92.40; H, 7.60. Found: C, 92.67, H, 7.20.

5. 3-Ethynylperylene and **I-M$_{31}$-(*t*-Bu)$_{32}$** were reacted using the general coupling procedure, and the product was purified by column chromatography eluting with 8% CH_2Cl_2/hexane to 13% CH_2Cl_2/hexane.[41] Yield 70%. ^{1}H NMR (400 MHz, $CDCl_3$) δ 8.33−8.09 (m, 5H), 7.89−7.55 (m, 48H), 7.53−7.31 (m, 51H), 1.34 (s, 288H). ^{13}C NMR (100 MHz, $CDCl_3$) δ 150.89, 134.67, 134.57, 134.47, 134.38, 133.90, 127.48, 125.94, 124.34, 123.85, 123.74, 123.62, 123.30, 123.11, 121.68, 91.79, 89.38, 89.02, 88.81, 88.47, 86.56, 34.81, 31.30. MS (MALDI) calcd for $C_{396}H_{392}$ 5151.5, found 5146.9. Anal. Calcd for $C_{396}H_{392}$: C, 92.33; H,7.67. Found: C, 92.10; H, 7.35.

6. 3-Ethynylperylene and **I-M$_{63}$-(*t*-Bu)$_{64}$** were reacted using the general coupling procedure, and the product was purified by column chromatography eluting with 8% CH_2Cl_2/hexane to 15% CH_2Cl_2/hexane.[41] Yield 65%. ^{1}H NMR (400 MHz, $CDCl_3$) δ 8.28−8.03 (m, 5H), 7.77−7.48 (m, 93H), 7.47−7.30 (m, 102H), 1.34 (s, 576H). ^{13}C NMR (100 MHz, $CDCl_3$) δ 150.85, 134.51, 134.46, 134.35,133.88, 125.94, 125.79, 124.32, 123.83, 123.73, 123.29, 123.07, 121.70, 91.79, 89.38, 88.87, 88.80, 88.48, 86.56, 34.78, 31.29. MS (MALDI) calcd for $C_{780}H_{776}$ 10 150.7. Found 10 202.5.

7. 3-Ethynylperylene and **I-M$_{127}$-(*t*-Bu)$_{128}$** were reacted using the general coupling procedure, and the product was purified by column chromatography eluting with 8% CH_2Cl_2/hexane to 15% CH_2Cl_2/hexane to give a bright yellow solid.[41] Yield 60%. ^{1}H NMR (400 MHz, $CDCl_3$) δ 7.76−7.27 (br m, aromatic H), 1.38−1.12 (br s, *tert*-butyl H), integral ratio of *tert*-butyl H to aromatic H calcd 2.93, found 3.22. ^{13}C NMR (100 MHz, $CDCl_3$) δ 150.78, 134.45, 134.40, 134.37, 134.25, 133.84, 127.49, 125.91, 124.28, 123.57, 123.30, 123.00, 121.73, 113.08, 95.43, 91.78, 86.60, 34.74, 31.27. MS (MALDI) calcd for $C_{1548}H_{1544}$ 20 149, found 20 120.

Phenyl-Terminated Monodendrons. 8. (3,5-Di-*tert*-butylphenyl)-acetylene and monodendron **I-M$_3$-(*t*-Bu)$_4$** were reacted using the general coupling procedure, and the product was purified by column chromatography eluting with hexane to give a white amorphous powder.[41] Yield 82%. ^{1}H NMR (400 MHz, benzene-d_6) δ 7.81 (s, 3H), 7.67 (d, J = 2 Hz, 6H), 7.52 (t, J = 1.9 Hz, 3H), 1.24 (s, 54H). ^{13}C NMR (100 MHz, $CDCl_3$) δ 150.88, 133.85, 125.94, 124.13, 123.05, 121.78, 91.48, 86.75, 34.83, 31.32. MS (FAB) calcd for $C_{54}H_{66}$ 715.06, found 714.4. Anal. Calcd for $C_{54}H_{66}$: C, 90.70, H, 9.30. Found: C, 90.28, H, 8.96. MS (EI) calcd for $C_{22}H_{26}$ 715.2, found 714.4.

9. (3,5-Di-*tert*-butylphenyl)acetylene and monodendron **I-M$_7$-(*t*-Bu)$_8$** were reacted using the general coupling procedure, and the product was purified by column chromatography eluting with 2% CH_2Cl_2/hexane to 5% CH_2Cl_2/hexane to give a white amorphous powder.[41] Yield 84%. ^{1}H NMR (400 MHz, benzene-d_6) δ 7.83 (t, J = 1.5 Hz, 2H), 7.77 (d, J = 1.4 Hz, 4H), 7.75 (d, J = 1.4 Hz, 2H), 7.74 (d, J = 1.4 Hz, 2H), 7.70 (d, J = 1.5 Hz, 8H), 7.65 (t, J = 1.5 Hz, 1H), 7.55−7.51 (m, 5H), 1.24 (s, 90H). ^{13}C NMR (100 MHz, $CDCl_3$) δ 150.91, 134.39, 133.90, 125.96, 124.44, 124.30, 123.63, 123.40, 123.19, 123.12, 121.70, 91.94, 91.74, 89.09, 88.71, 86.58, 34.83, 31.32. MS (FAB) calcd for $C_{102}H_{114}$ 1340.0, found 1339.7. Anal. Calcd for $C_{102}H_{114}$: C, 91.42; H, 8.58. Found: C, 91.14; H, 8.42.

10. (3,5-Di-*tert*-butylphenyl)acetylene and monodendron **I-M$_{15}$-(*t*-Bu)$_{16}$** were reacted using the general coupling procedure, and the product was purified by column chromatography eluting with 4% CH_2Cl_2/hexane to 9% CH_2Cl_2/hexane to give a white amorphous powder.[41] Yield 79%. ^{1}H NMR (400 MHz, benzene-d_6) δ 7.85 (d, J = 1.5 Hz, 2H), 7.84 (t, J = 1.5 Hz, 4H), 7.81 (d, J = 1.7 Hz, 8H), 7.78 (t, J = 1.4 Hz, 1H), 7.74 (d, J = 2 Hz, 2H), 7.72−7.67 (m, 22H), 7.54 (t, J = 1.7 Hz, 1H), 7.52 (t, J = 1.1.7 Hz, 8H), 1.24 (s, 162H). ^{13}C NMR (100 MHz, $CDCl_3$) δ 150.95, 150.92, 134.47, 134.39, 133.92, 127.49, 125.97, 124.35, 123.83, 123.73, 123.54, 123.33, 123.13, 121.70, 91.79, 89.35, 89.06, 88.74, 88.50, 86.56, 34.83, 31.32. MS (MALDI) calcd for $C_{198}H_{210}$ 2589.9, found 2589.4.

11. (3,5-Di-*tert*-butylphenyl)acetylene and monodendron **I-M$_{31}$-(*t*-Bu)$_{32}$** were reacted using the general coupling procedure, and the product was purified by column chromatography eluting with 8% CH_2Cl_2/hexane to 12% CH_2Cl_2/hexane to give a white amorphous powder.[41] Yield 89%. ^{1}H NMR (400 MHz, benzene-d_6) δ 7.85 (d, J = 1.5 Hz, 2H), 7.83 (t, J = 1.5 Hz, 8H), 7.81 (d, J = 1.7 Hz, 18H), 7.80−7.78 (m, 4H), 7.76 (t, J = 1.5 Hz, 1H), 7.73 (d, J = 1.5 Hz, 8H), 7.71 (d, J = 1.5 Hz, 2H), 7.70−7.67 (m, 36H), 7.51 (t, J = 1.5 Hz, 17H), 1.24 (s, 306H). ^{13}C NMR (100 MHz, $CDCl_3$) δ 150.89, 134.46, 134.36, 133.90, 127.49, 125.95, 124.33, 123.84, 123.30, 123.11, 121.68, 91.78, 89.37, 88.47, 86.55, 34.81, 31.30. MS (MALDI) calcd for $C_{390}H_{402}$ 5090, found 5102.

12. (3,5-Di-*tert*-butylphenyl)acetylene and monodendron **I-M$_{63}$-(*t*-Bu)$_{64}$** were reacted using the general coupling procedure, and the product was purified by column chromatography eluting with 8% CH_2Cl_2/hexane to 14% CH_2Cl_2/hexane to give a white amorphous powder.[41] Yield 70%. ^{1}H NMR (400 MHz, benzene-d_6) δ 7.95−7.87 (m, 7H), 7.86−7.80 (m, 56H), 7.79−7.73 (m, 22H), 7.72−7.65 (m, 72H), 7.61−7.58 (m, 2H), 7.49 (t, J = 1.5Hz, 33H), 1.24 (s, 594H). ^{13}C NMR (100 MHz, $CDCl_3$) δ 150.85, 134.51, 134.46, 133.88, 127.50, 125.93, 125.87, 125.79, 124.32, 123.82, 123.69, 123.29, 123.13, 123.08, 121.70, 91.79, 89.38, 88.48, 86.56, 34.79, 31.29. MS (MALDI) calcd for $C_{774}H_{786}$ 10 089, found 10 078.

13. (3,5-Di-*tert*-butylphenyl)acetylene and monodendron **I-M$_{127}$-(*t*-Bu)$_{128}$** were reacted using the general coupling procedure, and the product was purified by column chromatography eluting with 8% CH_2Cl_2/hexane to 20% CH_2Cl_2/hexane to give a white amorphous powder.[41] Yield 65%. ^{1}H NMR (400 MHz, benzene-d_6) δ 7.98−7.38 (br m, aromatic H), 1.37−1.04 (br s, *tert*-butyl H), integral ratio of *tert*-butyl to aromatic H, calcd 3.04, found 3.73. ^{13}C NMR (100 MHz, $CDCl_3$) δ 150.78, 134.42, 134.29, 133.85, 127.49, 126.12, 126.10, 125.91, 124.29, 123.79, 123.75, 123.67, 123.65, 123.60, 123.30, 123.10, 123.06, 123.01, 121.73, 91.79, 89.37, 88.87, 88.53, 86.59, 34.74, 31.27. MS (MALDI) calcd for $C_{1542}H_{1554}$ 20 087, found 20 177.

Acknowledgment. We dedicate this paper to Professor Nelson Leonard, a figure of scholarly excellence, on his 80th birthday. We thank Professor Devens Gust, Arizona State University, for helpful discussions, Professor R. Kopelman, University of Michigan, for encouraging this study, and the Office of Naval Research (Grant N00014-94-I-0639) and the National Science Foundation (Grant DMR 95-20402) for financial support.

JA961418T